OPTICAL AND THERMAL ANALYSIS OF ALL-GLASS FLAT PLATE SOLAR COLLECTOR FOR DOMESTIC APPLICATIONS

Raquel M. Carvalho
Mavd P. R. Teles
Fátima A. M. Lino
Kamal A. R. Ismail
raquel.miguezcarvalho@gmail.com
mavd.ribeiro@hotmail.com
fatimalino@fem.unicamp.br
kamal@fem.unicamp.br
University of Campinas, Faculty of Mechanical Engineering, Department of Energy, Mendeleiev street, 200, Cidade Universitária "Zeferino Vaz", Barão Geraldo, Postal Code 13083.860, Campinas (SP), Brazil

Abstract. *The challenge of this century is to find new sustainable energy sources that impact less the environment during generation and utilization. Solar and wind energy appear at the top of the list of renewable energies of high potential, widely available, of dominated technology and well accepted. Thermal comfort and hot water are responsible for the distortion of the electricity demand curves, management difficulties and high cost. These energy demands can be attended by available solar energy technologies. This paper presents the optical and thermal analysis of a novel all-glass flat plate solar collector which can produce hot water and increase passive thermal comfort. The bottom glass external surface is reflective. Water is used as the working fluid. The collector has a length and width of 2000 and 1000 mm, respectively. The numerical thermal analysis was performed using the SIMPLE algorithm. The collector inclination angle and five different mass flow rates are considered to investigate the effect on the outlet fluid temperature and the thermal efficiency of the collector.*

Keywords: *All-glass flat plate solar collector, Solar energy, Numerical model, Renewable energy, Passive thermal comfort*

1 INTRODUCTION

Due to growing energy demands, solar energy is been looked at as a viable source of energy. Solar collector has been greatly studied. Many of the new designs have been developed to improve the thermal performance of flat plate collectors (Pandey & Chaurassiya, 2017). Studies focused finding the optimum gap between the glass sheets, to decrease the heat loss of the flat plate.

Siegel (1973) used the net radiation method to calculate the radiation transmission through a glass plate with a water layer adjacent to it. This method requests simple equations at each interface to solve complicated systems as those involving combinations of absorbing and non-absorbing layers. Threlkeld (1970) analyzed the effect of solar radiation in different materials, including the heat transmission through diathermanous materials.

Pandey & Chaurassiya, (2017) presented a review on the analysis and development of flat plate collectors. Based on his review he concluded that there is a decrease in efficiency with the decrease in volume flow rate of the nanofluid, beside improvements of the heat transfer, characterizing gains. Another conclusion is the increase the heat absorbed from solar radiation, but the absorber must be capable to absorb different wavelengths effectively. He also concluded that the heat loss reduction increase the efficiency due to decrease heat loss, but the technique used must be cost-effective. He concluded that employing PCM with paraffin eliminates need for storage units making water heating systems less bulky. High density, small volume change, low vapor pressure, chemically stability and cost effective.

Tagliafico et al. (2014) investigated the dynamic thermal models and CFD analysis for flat-plate thermal solar and concluded that the steady state model turns out to be an easy computational model, efficient and adequate to predict the energy yield of the solar collector as far as a long-time averaged performance (e.g., monthly) is required. In this sense, it is suitable for feasibility studies and for preliminary system design. Moreover, the steady state approach has a good performance also in the short-period (e.g., daily), only if the variations of the climatic conditions (mainly the solar radiation) are smooth.

A theoretical study on the optimum tilt angle for flat plate collectors was developed by Stanciu and Stanciu (2014), and concluded that the optimum tilt angle for a flat plate collector should be computed as function on the latitude and declination.

This paper presents the optical, thermal and fluid-dynamic analysis of a novel all-glass flat plate solar collector which can be used as a conventional double glass window or skylight window with fluid circulation to produce hot water and increase passive thermal comfort. The bottom glass external surface is reflective. Water is used as the working fluid. The collector has a length and width of 2000 and 1000 mm, respectively. The numerical thermal analysis was performed using the SIMPLE algorithm which uses the governing equations (continuity, momentum, and energy) for perform the calculations. The collector inclination angle is varied to five different flow rates are considered to investigate their effects, the outlet fluid temperature and the thermal efficiency of the collector.

2 OPTICAL ANALYSES

2.1 All-glass flat plate solar collector model parameters

The All-glass flat plate solar collector model is composed of two glass sheets separated by a water gap and the bottom glass external surface is reflective as is shows in Fig. 1. The reflective film considered in this work is ideal and has a reflectance index equal to one. Water is used as the working fluid. The collector has a length, width and thickness (gap between the gasses) of 2000, 1000 and 5 mm, respectively.

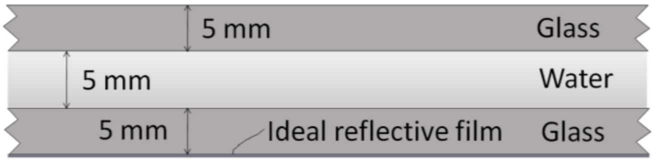

Figure 1. All-glass flat plate solar collector

2.2 Incidence angle and orientation of the collector

According to Kreith and Kreider (1978) the orientation angles of the collector denominated as β (collector slope angle) and a_w (collector's azimuth); are dependent on the solar angles: δ_s (declination angle of the sun), h_s (solar hour angle), La (latitude), a_s (sun azimuth) and i (incidence angle). They can be related by Eq. (1):

$$\cos(\mathrm{i}) = \mathrm{sen}(\delta_s)(\mathrm{sen(La)}\cos(\beta) - \cos(\mathrm{La})\mathrm{sen}(\beta)\cos(a_w)) + \cos(\delta_s)\cos(h_s)(\cos(\mathrm{La})\cos(\beta) + \mathrm{sen(La)}\mathrm{sen}(\beta)\cos(a_w)) + \cos(\delta_s)\mathrm{sen}(\beta)\mathrm{sen}(a_w)\mathrm{sen}(h_s). \quad (1)$$

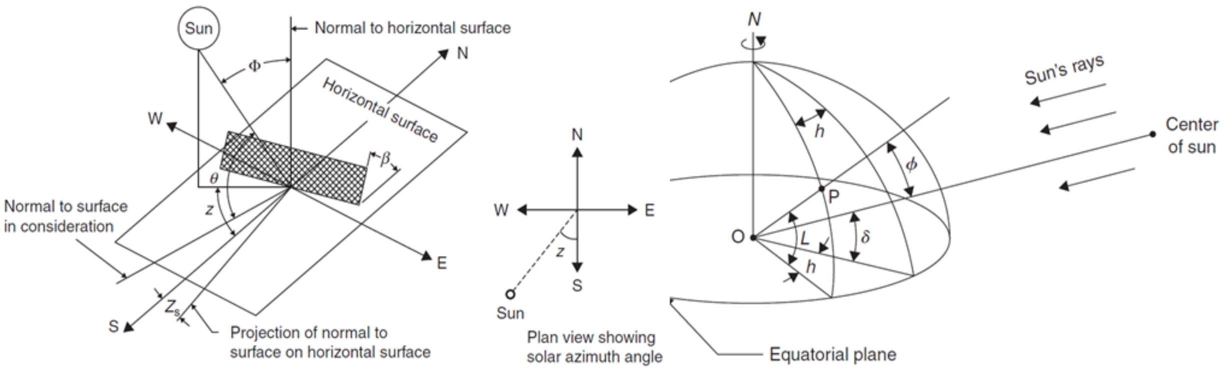

Figure 2. Definition of angles: β, a_w, δ_s, h_s, La, a_s and i

Source: Adapted from Kalogirou (2014)

To determine the inclination angle of the collector, knowledge of the other angles is necessary. The declination angle is determined according to the date and time of the year;

hence, it is necessary to choose the date for the location of the solar collector. The choice of this date was made according to the dates of maximum incidence of solar irradiation and with the minimum variation of solar elevation. According to Rapp (1981) for east-west orientation the days for which the focus remains constant all day are in the first day of autumn and spring. According to the data from Crescesb/Cepel (2017) the solar irradiation for the city of Campinas for the horizontal and inclined surfaces is shown in Fig. 2.

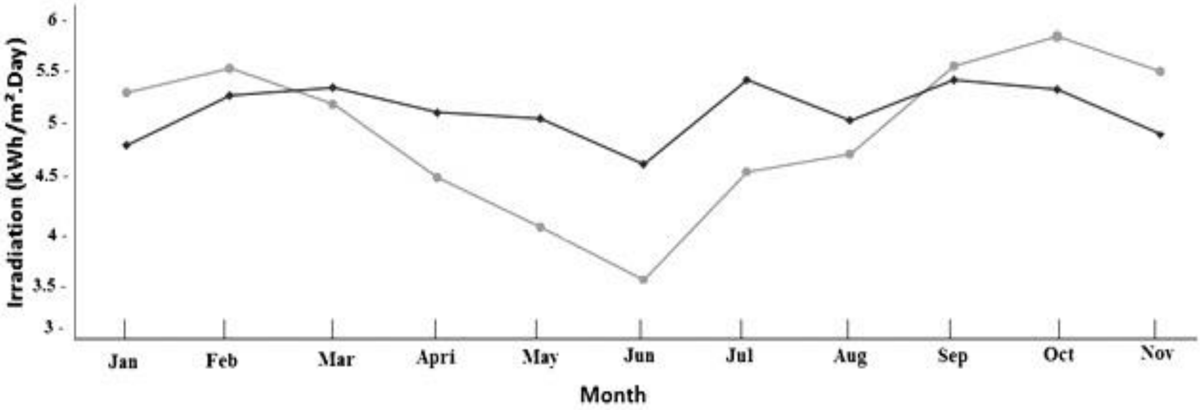

Figure 3. Solar incidence in the city of Campinas with horizontal and inclined plane

Source: Adapted from Crescesb/Cepel (2017)

The spring and autumn seasons of the year 2017 for Brazil occurred on the dates September 22nd and March 20th, respectively (INMET 2017). From these data the chosen date for the city of Campinas is September 22nd, 2017 at solar noon. For this date, according to Nautical Almanac of the Stars (2017), the declination angle of the sun is δ_s = 0 ° 7.8 '.

Thus, using a_w = 0º, the best slope angle of the collector was calculated for one of the highest incidence dates for Campinas, which is close to the latitude value as shown below.

Best value of β for on September 22 at noon:

$$a_w = 0^o, \delta_s = 0.1167^o, i = 0^o, h_s = 0^o$$
$$\beta = -22.58^o, La = -22.53^o$$

Where I_b is the incident solar radiation.

Figure 1 shows that the direct solar radiation intercepted by the flat plate solar collector is related by Eq. (2):

$$I_{b,c} = I_b \cos(i). \tag{2}$$

Since it is possible to determine the angle of incidence of the collector throughout the day for each period of the day and the year, one can calculate the percent of intercepted direct solar radiation. The most relevant collector slope angles are simulated for September 22nd at the city of Campinas-SP in Fig. 3. The slope angles with highest interceptions are respectively: β=22.58°, β=0° and β=45º.

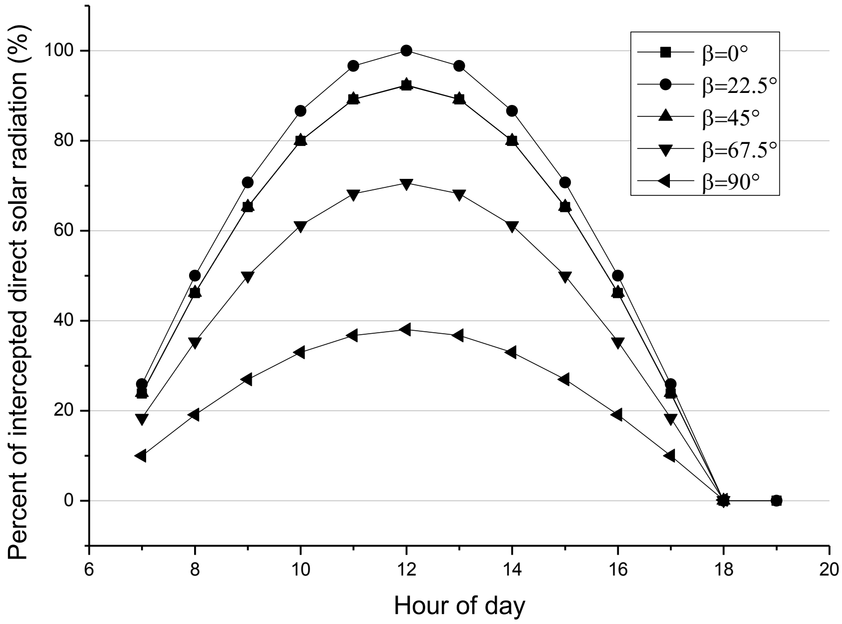

Figure 4. Percentage of intercepted solar radiation; for relevant periods of the year, Campinas (SP)

3 THERMAL ANALYSIS

3.1 The mathematical model and numerical treatment

The algorithm used in this work to calculate the flow field and the variation of temperature in a two-dimensional grid is the SIMPLE algorithm. It uses the finite volume method and its operation is described in Patankar (1980). The results are for the mid width, disregarding the walls' and boundaries' effects of this direction.

This algorithm uses three kinds of grids. The first grid has control volumes for the internal and boundary points and it stores temperature and properties. The second and third grids are staggered and stores velocity in *x* and *y* directions respectively.

The collector is very long in *x* direction, this implies in significant changes near to the walls and small changes in the middle. For this reason, the grid was stretched in the x-direction by a hyperbolic tangent function.

The governing differential equations for constant density and viscosity used are:

$$\frac{\partial u}{\partial x}+\frac{\partial v}{\partial y}=0. \tag{3}$$

Proceedings of the XXXVIII Iberian Latin-American Congress on Computational Methods in Engineering
P.O. Faria, R.H. Lopez, L.F.F. Miguel, W.J.S. Gomes, M. Noronha (Editores), ABMEC, Florianópolis, SC, Brazil, November 5-8, 2017.

$$\rho\frac{\partial u}{\partial t}+\rho u\frac{\partial u}{\partial x}+\rho v\frac{\partial u}{\partial y}=\mu\left(\frac{\partial^2 u}{\partial x^2}+\frac{\partial^2 u}{\partial y^2}\right)-\frac{\partial p}{\partial x}. \tag{4}$$

$$\rho\frac{\partial v}{\partial t}+\rho u\frac{\partial v}{\partial x}+\rho v\frac{\partial v}{\partial y}=\mu\left(\frac{\partial^2 v}{\partial x^2}+\frac{\partial^2 v}{\partial y^2}\right)-\frac{\partial p}{\partial y}. \tag{5}$$

$$\rho\left(u\frac{\partial T}{\partial x}+v\frac{\partial T}{\partial y}\right)=\frac{\partial}{\partial x}\left(\frac{k}{c_p}\frac{\partial T}{\partial x}\right)+\frac{\partial}{\partial y}\left(\frac{k}{c_p}\frac{\partial T}{\partial y}\right)+S. \tag{6}$$

The source-term (S) in this study is the solar direct radiation. For glass, as it is a diathermanous material, the part of the incidence radiation that will be absorbed by the glass will be calculated by the following equations, (Threlkeld, 1970):

$$\alpha_\kappa=1-r-\frac{(1-r)^2 a}{1-ra}. \tag{7}$$

Where, α_κ is the absorptance for a monochromatic radiation, r is the specular reflectivity for single radiation component, the subscript 1 is for the first change of environment (air-glass) and 2 is the second (glass-water) and a is the absorption coefficient. Both r and a are calculated as:

$$r_1=\left[\frac{n_2-n_1}{n_2+n_1}\right]^2. \tag{8}$$

$$a=e^{-\kappa L'}. \tag{9}$$

Where κ is the extinction coefficient, n is the index of refraction, the subscript 1 is for air, 2 is glass, and 3 is water and L' is:

$$L'=\frac{L}{\sqrt{1-\frac{\sin^2 i}{n_1^2}}}. \tag{10}$$

Where, L is the thickness of the glass and i is the incidence angle.

In this study water is considered a non-participating medium in the direct radiation.

The source-term for the glass volumes is:

$$S=\alpha_\kappa I. \tag{11}$$

The boundary condition is the air free convection of the wind for the north and south surfaces, west and east are considered adiabatic and are related by the following equations, respectively:

$$-k\left.\frac{\partial T}{\partial y}\right|_{y=M1} = h_{conv-amb}\left(T_{ext} - T_{M1}\right). \tag{12}$$

Where, k is the thermal conductivity, T_{M1} is the temperature at the north boundary and T_{ext} is the ambient temperature.

$$-k\left.\frac{\partial T}{\partial y}\right|_{y=1} = h_{conv-amb}\left(T_{ext} - T_{1}\right). \tag{13}$$

Where, T_1 is the temperature at the south boundary and, T_2 is the temperature of the first control volume internal point in x direction.

$$T_1 = T_2\,. \tag{14}$$

$$T_{L1} = T_{L2}\,. \tag{15}$$

Where, T_{L2} is the temperature of the last control volume internal point in x direction.

These boundary conditions are treated in the adjacent control volume internal point as an additional source term.

According to Kreith and Bohn (2003), the natural heat transfer convection in glass wall for flat surfaces can be estimated by the correlation:

$$\bar{h}_{conv-amb} = \left(0.036\mathrm{Pr}^{1/3}\,\mathrm{Re}_L^{0.8}\right)\frac{k_{air}}{L}. \tag{16}$$

Where, Pr is the Prandtl number, Re is the Reynolds number, k_{air} is the thermal conductivity and L is the collector length.

3.2 Validation

The Net-Radiation Method is an analytical tool that can be used to derive the radiation characteristics. In this paper, it was used to verify the accuracy of the simulation, by calculating the absorptance for an all-glass flat plate solar collector with and without reflective surface.

The two different situations and the outgoing and incoming energy at each interface are illustrated in Figs. 4 and 5. The following energy for the case without reflective film equations are (Siegel, 1973):

$$q_{o,1} = r_1 q_{i,1} + \left(1 - r_1\right) q_{i,2}\,. \tag{17a}$$

$$q_{o,2} = (1 - r_1)q_{i,1} + r_1 q_{i,2}\,. \tag{17b}$$

$$q_{o,3} = r_2 q_{i,3} + (1 - r_2)q_{i,4}\,. \tag{17c}$$

$$q_{o,4} = (1 - r_2)q_{i,3} + r_2 q_{i,4}\,. \tag{17d}$$

$$q_{o,5} = r_3 q_{i,5} + (1 - r_3)q_{i,6}\,. \tag{17e}$$

$$q_{o,6} = (1 - r_3)q_{i,5} + r_3 q_{i,6}\,. \tag{17f}$$

$$q_{o,7} = r_4 q_{i,7} + (1 - r_4)q_{i,8}\,. \tag{17g}$$

$$q_{o,8} = (1 - r_4)q_{i,7} + r_4 q_{i,8}\,. \tag{17h}$$

The reflective film is considerate as an ideal reflector, hence for the system with mirror, $q_{o,8}$ is equal 0, and the energy equations are presented below.

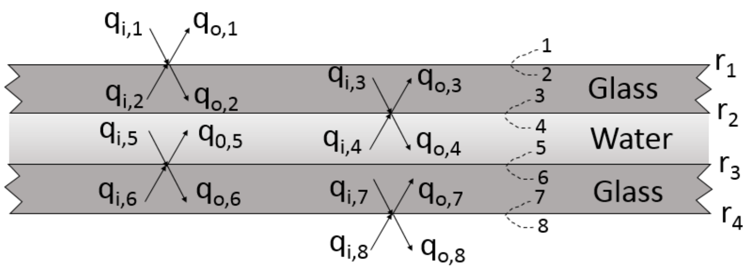

Figure 5. All-glass flat plate solar collector without reflective film

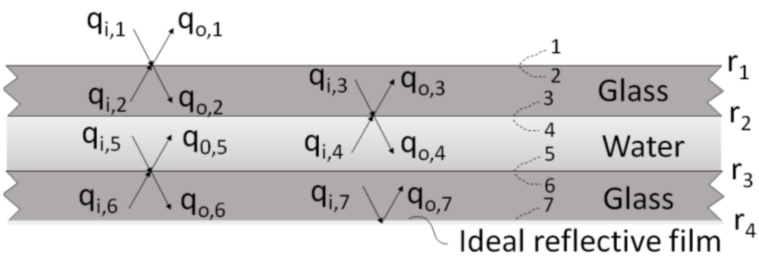

Figure 6. All-glass flat plate solar collector with reflective film

$$q_{i,1} = q\,. \tag{18a}$$

$$q_{i,2} = (1 - \alpha_1)q_{o,3}\,. \tag{18b}$$

Proceedings of the XXXVIII Iberian Latin-American Congress on Computational Methods in Engineering
P.O. Faria, R.H. Lopez, L.F.F. Miguel, W.J.S. Gomes, M. Noronha (Editores), ABMEC, Florianópolis, SC, Brazil, November 5-8, 2017.

$$q_{i,3} = (1-\alpha_1)q_{o,2}\,. \tag{18c}$$

$$q_{i,4} = q_{o,5}\,. \tag{18d}$$

$$q_{i,5} = q_{o,4}\,. \tag{18e}$$

$$q_{i,6} = (1-\alpha_2)q_{o,7}\,. \tag{18f}$$

$$q_{i,7} = (1-\alpha_2)q_{o,6}\,. \tag{18g}$$

$$q_{i,8} = 0. \tag{18h}$$

Where r and α are calculated as in Eqs. (7) and (8), respectively. The absortance is calculated as a function of the incidence angle. Thus, it is calculated for various slope angles and for the variation of the declination solar angle during a year.

According to Kreith and Kreider (1978) the variation of the declination solar angle occurs in this to extremes latitudes, the tropic of cancer ($23\frac{1}{2}$ ° N) and Capricorn ($23\frac{1}{2}$ ° S), where the sun reaches the earth at least once a year. Figure 7 (a,b) shows the results of the absorptance for these conditions.

Finally, the absorptance of the system with and without reflective film is calculated as:

$$\alpha = 1-\left(\frac{q_{o,8}}{q}+\frac{q_{o,1}}{q}\right). \tag{19}$$

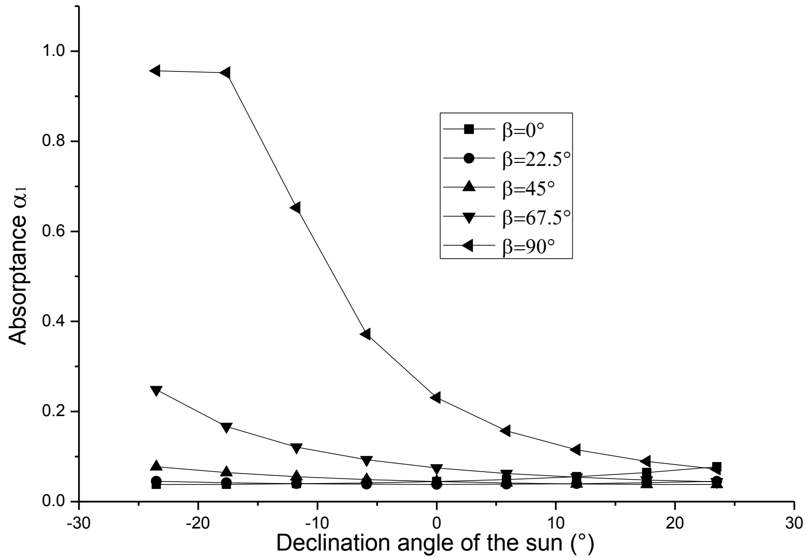

[a] β=0°,β=22.58°, β=45°, β=67.5° and β=90°

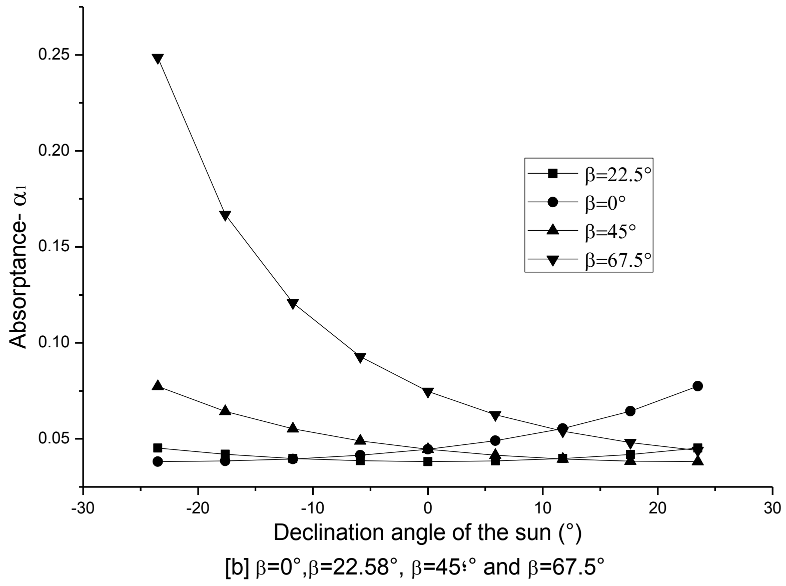

Figure 7 (a,b). Absorptance for different slopes angles

The Net-Radiation Method includes the effects of radiation transfer. Therefore, to validate the algorithm it was necessary initially to use just a radiation transfer in order to have the same terms for comparison. Fig. 8 shows the comparison between the analytical and the numerical results of the all-glass flat plate collector with and without reflector film, for various slope angles of the collector and for incident solar radiation of the representative day of October at noon.

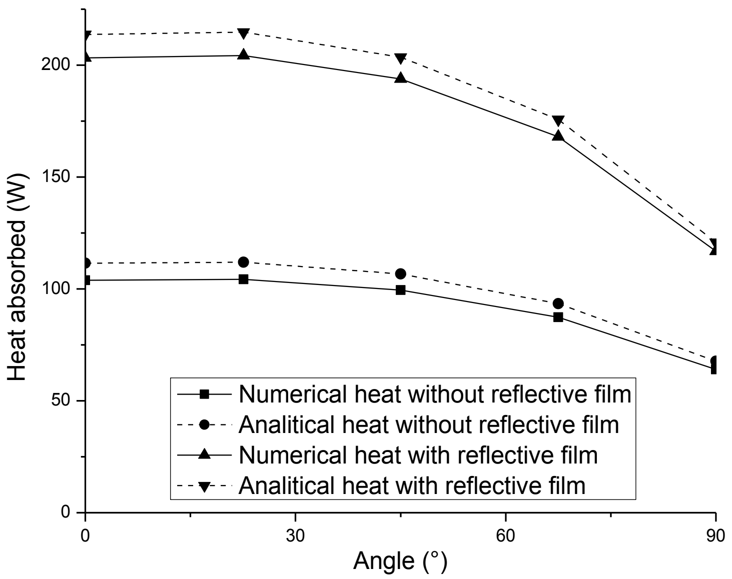

Figure 8. Comparison between analytical and numerical results with and without reflective film

The comparison of the performance between the numerical model and the analytical model is shown in Table 1. A good correlation has been obtained for the thermal efficiencies of the simulated slope angles. The maximum error is about 6.86%.

Table 1. Comparison between analytical and numerical results without natural heat transfer convection*

Reflective film	β	Ib,c (W/m^2)	T_{outlet} (°C)	Q_{num} (W)	η (%)	α_λ	Q_{ana} (W)	% Error (num – ana)
with	0°	732.264	34.68	203.288	13.88	0.145894	213.666	4.86
without	0°	732.264	29.96	103.840	7.09	0.076115	111.472	6.85
with	22.58°	742.637	34.74	204.268	13.75	0.144564	214.717	4.87
without	22.58°	742.637	29.96	104.294	7.02	0.075387	111.971	6.86
with	45°	640.262	34.24	193.855	15.14	0.158952	203.542	4.76
without	45°	640.262	29.76	99.448	7.77	0.083289	106.654	6.76
with	67.5°	440.245	32.98	167.989	19.08	0.199580	175.728	4.40
without	67.5°	440.245	29.16	87.331	9.92	0.106037	93.364	6.46
with	90°	173.204	30.56	116.829	33.73	0.348699	120.792	3.28
without	90°	173.204	28.06	63.986	18.47	0.195511	67.726	5.52

* Table 1 is calculated or flow rate= 0.005 (L/s), ambient temperature= 25°C.

Where, η is the efficiency, T_{amb} is the temperature inlet of the water, T_{outlet} is the average of the outlet temperature of the water, Q_{num} is the total of heat absorbed by the collector numerically calculated, and Q_{ana} is the total heat absorbed by the collector analytically calculated.

4 RESULTS AND DISCUSSION

In section 3, the all-glass flat plate collector numerical model was described and validated. Thus, to approximate the numerical model to a real case was included the phenomenon of natural heat transfer convection in the collector. This additional boundary condition was described in section 3.1. Figure 9 shows the variation of the heat absorbed by the flat plate for different slope angles with and without reflective film for an incidence solar radiation of the representative day of October at noon.

The addition of the reflective film in the all-glass flat plat solar collector increased the heat absorbed and the efficiency. The smallest and the highest efficiency are respectively for: β=22.58° and β=90° slope angles. This shows that the absorptance increased with the increase of the slope angle. However, the maximum heat absorbed by the collector is for 22.58 slope angle. This is due to the fact that radiation intercepted by the collector is function of the incidence angle. For high values of slope angles, there is less radiation intercepted by the collector. Table 2 shows the results for the tests with and without reflective film and for the different slope angles, with natural heat transfer convection.

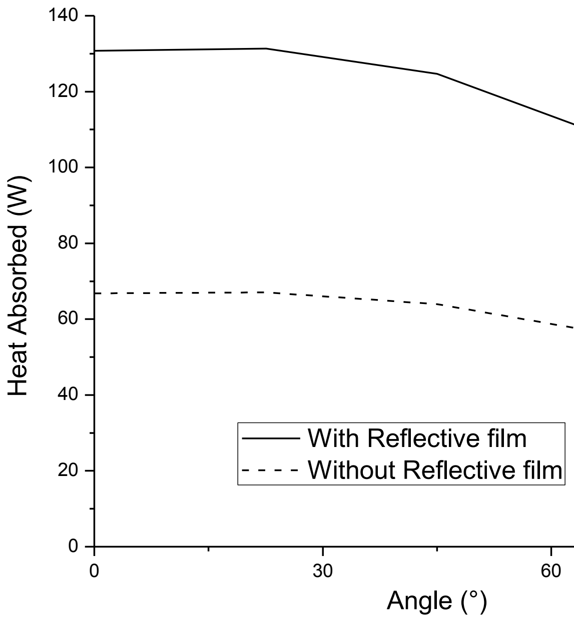

Figure 9. Heat absorber by the flat plate with and without reflective film for various slopes angles

Table 2. All-glass flat plate solar collector with and without reflective film, with natural heat transfer convection*

Reflective film	β	Ib,c (W/m²)	Tout (°C)	Qnum (W)	η (%)
with	0°	732.264	31.26	130.74202	8.93
without	0°	732.264	28.18	66.784256	4.56
with	22.58°	742.637	31.26	131.371979	8.84
without	22.58°	742.637	27.86	67.0766296	4.52
with	45°	640.262	30.96	124.675583	9.74
without	45°	640.262	28.06	63.9597931	4.99
with	67.5°	440.245	30.16	108.039948	12.27
without	67.5°	440.245	27.68	56.1665878	6.38
with	90°	173.204	28.56	75.1380997	21.69
without	90°	173.204	29.36	41.1530266	11.88

*Table 2 is calculated for flow rate= 0.005 (kg/s), ambient temperature= 25°C, natural heat transfer convection coefficient= 4.48(W/(m²K)) and wind spend= 9.44 (m/s).

As the maximum heat absorbed by the collector was for 22.58 slope angle, this angle was used to calculate for the representative days of the other months as is shown in Fig. 10. Changing the velocity of the water, four more mass flow rates are calculated to compare the exit fluid temperature and the thermal efficiency of the collector. To ensure that the system is in a laminar flow regime, Reynolds must be less than 2300. Reynolds is calculate by Çengel and Ghajar (2012):

$$\mathrm{Re} = \frac{VD_h}{\nu}. \tag{20}$$

Where V is the average velocity, ν is the kinematic viscosity and D_h is the hydraulic diameter and is calculated by:

$$D_h = \frac{2ab}{a+b}. \tag{21}$$

Where a is the height and b is the width of the channel where water flows.

The average velocity must be less than 0.1856 m/s to obtain a laminar flow.

The temperature along the flat plate with reflective film for 22.58° slope angle with 0.005 kg/s flow rate is shown in Fig. 11. The different velocities and mass flow rates are present in Table 3. Table 4 shows the results for the tests different mass flow rates with and without reflective film with natural heat transfer convection for 22.58° slope angle.

Table 3. Velocity and mass flow rate

Velocity $*10^{-5}$ (m/s)	Mass flow rate (kg/s)
80.2407	0.004
100.3009	0.005
120.3611	0.006
140.4213	0.007
160.4814	0.008

Table 4. Heat absorber for different mass flow rates*

Reflective film	Mass flow rate (kg/s)	T_{out} (°C)	Heat lost (convection) (W)	Q_{num} (W)	η (%)
with	0.004	31.86	89.00495	114.7142	7.72
without	0.004	28.48	45.44614	58.57446	3.94
with	0.005	31.26	76.71658	131.372	8.84
without	0.005	28.2	39.16977	67.07663	4.52
with	0.006	30.72	67.3979	143.4173	9.66
without	0.006	27.9	34.41757	73.23705	4.93
with	0.007	30.2	60.07201	152.327	10.26
without	0.007	27.66	30.6723	77.77824	5.24
with	0.008	29.76	54.19719	159.1929	10.72
without	0.008	27.4	27.67466	81.28945	5.47

* Table 4 is calculated for solar radiation= 742.6373 (W/m²), inlet temperature and ambient temperature= 25°C, natural heat transfer convection coefficient= 4.48(W/(m²K)).

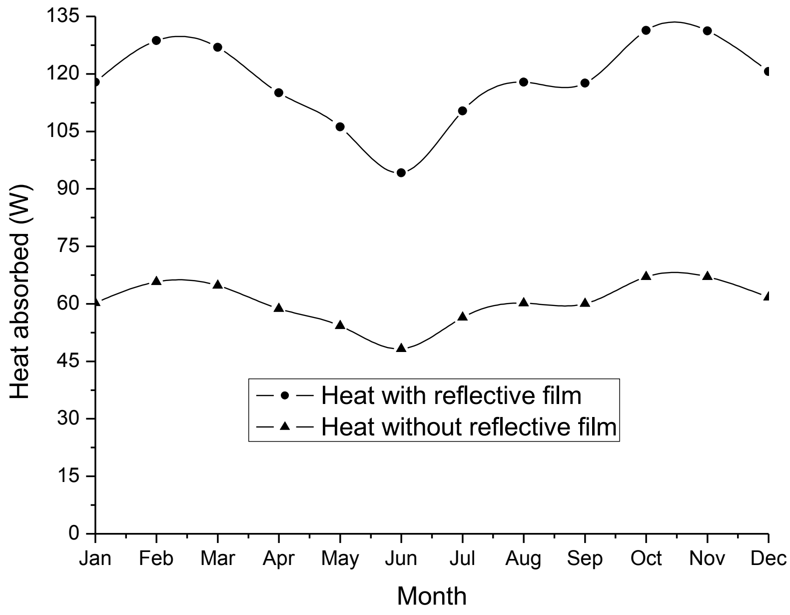

Figure 10. Heat absorber by the flat plate with and without reflective film for 22.58° slope angle during the year

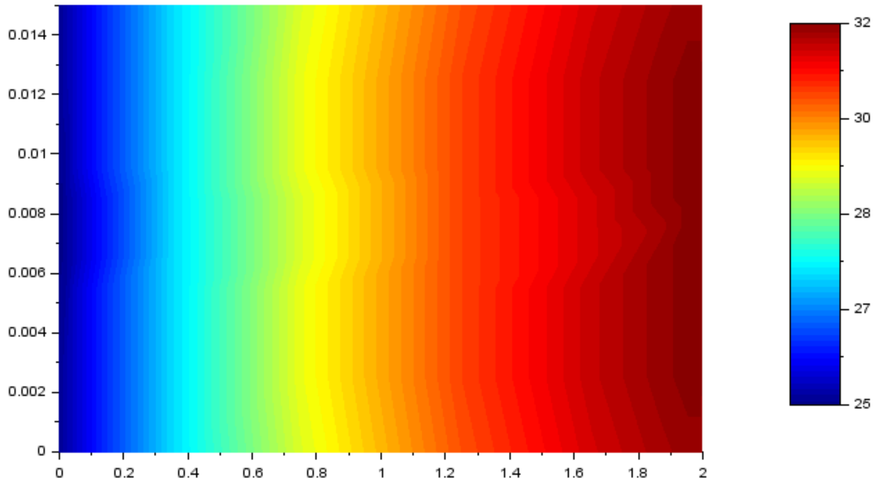

Figure 11. Temperature along the flat plate with reflective film for 22.58° slope angle with 0.005 kg/s flow rate

The input temperature of water is 25°C, as is represented in Fig. 11. As the water flow along the collector the temperature increases, until the greatest temperature as 32°C.

Figure 12 shows the variation of exit fluid temperature for different mass flow rates with and without reflective film for an incident solar radiation of the representative day of October at noon, and Fig. 13 shows the thermal efficiency of the collector.

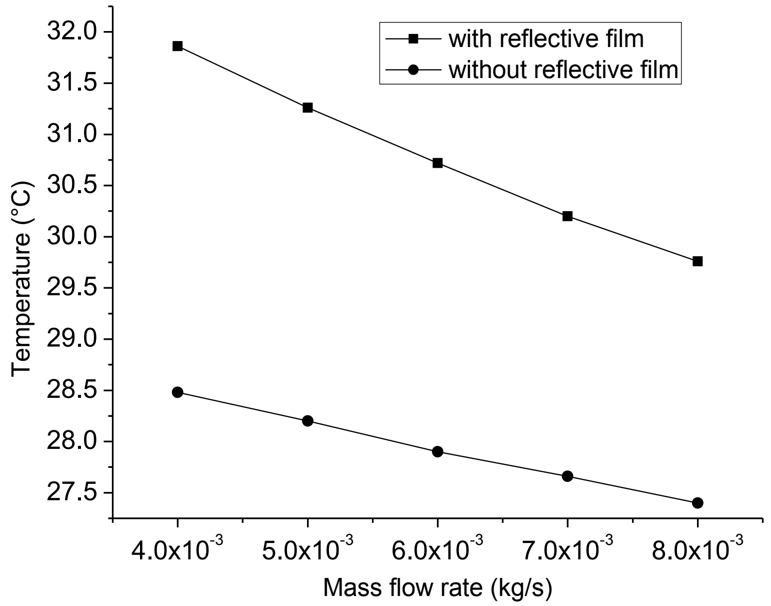

Figure 12. Outlet fluid temperature for different mass flow rates with and without reflective film

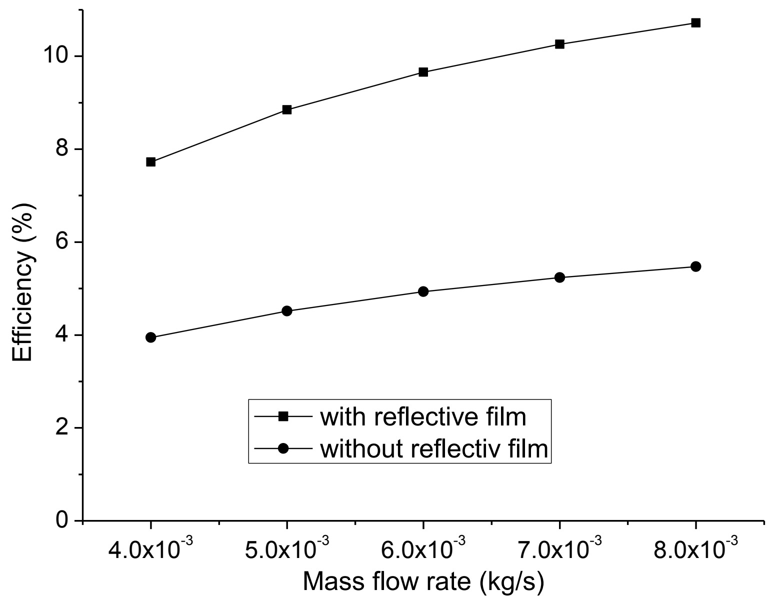

Figure 13. Thermal efficiency for different mass flow rates with and without reflective film

The outlet fluid temperature decreases linearly with the increase of the mass flow for both systems. The efficiency increases with the increase of the mass flow, because the heat lost with the convection is directly proportional to the temperature of the glass, as the temperature decreases, the heat lost also decreases, and this leads to increase the efficiency.

5 CONCLUSIONS

A mathematical model considering the optical, thermal and fluid dynamic aspects of an All-glass flat plate solar collector has been carried out. The accuracy of the detailed simulation model is demonstrated in this paper by comparison with the analytical method Net-Radiation for different slope angles. The maximum error obtained was 6.86%.

The numerical model is based on the application of governing equations and used general empirical correlations. The numerical model was simulated for different slope angles, flow rates and periods of year.

Comparing the different slope angles, 22.58° with south orientation has absorbed more heat than the others, however it had the smallest efficiency. The heat absorbed during the year was proportional to the direct incidence radiation.

Numerical results showed that the efficiency of the collector is direct proportional to the mass flow rate and the outlet temperature is inversely proportional. The mass flow rate should be chooses depending on the application, if a large amount of water is needed, the flow speed should be high and if the outlet temperature is important, the flow should be slow.

Acknowledgements

The authors wish to thank the CNPQ for the master scholarship for the first author, the FAPEMA for the master scholarship for the second author and the PQ Research Grant for the fourth author.

REFERENCES

Çengel, Y. A., Ghajar, A. J., 2012. *Transferência de Calor e Massa*. Mc Graw Hill.

Crescesb/Cepel, 2017. Available at: http://cresesb.cepel.br/index.php?section=sundata. Accessed in: February 07th, 2017.

Guerrero, J. R. H., 2002. *Modelagem e Análise de Janelas Térmicas.* PhDthesis, UNICAMP.

INMET, 2017. Available at:http://www.inmet.gov.br/portal/index.php?r=home2/page&page=estacoesDoAno. Accessed in: February 07th, 2017.

Ismail, K. A. R., Henríquez, J. R., 1998. U-Values, optical and thermal coefficients of composite glass systems. *Solar Energy Materials and Solar Cells*, vol. 52, pp. 155-182.

Kalogirou, S. A., 2014. Solar Energy Engineering: Processes and Systems. Elsevier Inc.

Kreith, F. & Bohn, M. S., 2003. *Principles of Heat Transfer*. Thomson Learning.

Kreith, F. & Kreider, J. F.,1978. *Principles of Solar Engineering*. Hemisphere Publishing Corporation.

Nautical Almanac of the Stars, 2017. Available at: https://www.nauticalalmanac.it/en/navigation-astronomy/the-nautical-almanac.html. Accessed in: February 08th, 2017.

Pandey, K. M., & Chaurasiya, R., 2017. A review on analysis and development of solar flat plate collector. *Renewable and Sustainable Energy Reviews*, 67, pp. 641-650.

Patankar, S. V., 1980. *Numerical Heat Transfer and Fluid Flow*. McGraw-Hill Book Company.

Rapp, D.,1981. *Solar Energy*. Prentice-Hall.

Siegel, R., 1973. Net Radiation Method for Transmission through Partially Transparent Plates. *Solar Energy*, vol. 15, pp. 273–276.

Stanciu, C., Stanciu, D., 2014. Optimum tilt angle for flat plate collectors all over the World – A declination dependence formula and comparisons of three solar radiation models. *Energy Conversion and Management*, 81, pp.133–143.

Tagliafico, L.A., Scarpa, F. & De Rosa, M., 2014. Dynamic thermal models and CFD analysis for flat-plate thermal solar collectors - A review. *Renewable and Sustainable Energy Reviews*, 30, pp.526–537.

Threlkeld, J. L., 1970. *Thermal Environmental Engineering*. Prentice-Hall Inc.